International Journal of Nanomedicine

Dovepress
open access to scientific and medical research

Open Access Full Text Article

ORIGINAL RESEARCH

Combined Orobol-Bentonite Composite Formulation for Effective Topical Skin Targeted Therapy in Mouse Model

Duy-Thuc Nguyen[1], Min-Hwan Kim[1], Na-Young Yu[1], Min-Jun Baek[1], Kyung-Sun Kang[2], Ki Won Lee[3], Dae-Duk Kim[1]

[1]College of Pharmacy and Research Institute of Pharmaceutical Sciences, Seoul National University, Seoul, Republic of Korea; [2]Adult Stem Cell Research Center and Research Institute for Veterinary Science, College of Veterinary Medicine, Seoul National University, Seoul, Republic of Korea; [3]Department of Agricultural Biotechnology, Seoul National University, Seoul, Republic of Korea

Correspondence: Dae-Duk Kim, College of Pharmacy and Research Institute of Pharmaceutical Sciences, Seoul National University, Seoul, 08826, Republic of Korea, Tel +82-2-880-7870, Fax +82-2-873-9177, Email ddkim@snu.ac.kr

Purpose: Orobol is an isoflavone that has a potent skin protection effect. The objective of this study was to prepare a novel bentonite-based composite formulation of orobol to enhance topical skin delivery.

Methods: The composition was optimized based on the orobol content in the composite and the in vitro release studies, followed by the in vitro and in vivo hairless mouse skin deposition studies. Physicochemical characterizations of the composite formulation were performed by powder X-ray refractometry (XRD) and scanning electron microscopy (SEM). The in vitro cytotoxicity and in vivo toxicity studies were conducted in human keratinocytes and in hairless mouse, respectively.

Results and Discussions: The in vitro release of orobol from the bentonite composites was higher than that from the suspension, which was further increased with the addition of phosphatidylcholine. The composite formulation significantly enhanced the in vitro and in vivo skin deposition of orobol in hairless mouse skin compared to the orobol suspension. Moreover, the addition of phosphatidyl choline not only improved the dissolution and incomplete release of orobol from the bentonite composite but also enhanced the deposition of orobol in the skin. XRD histograms and SEM images confirmed that the enhanced dissolution of orobol from the composite was attributed to its amorphous state on bentonite. The in vitro and in vivo toxicity studies support the safety and biocompatibility of the orobol-loaded bentonite composite formulation.

Conclusion: These findings suggest that the orobol-loaded bentonite composite formulation could be a potential topical skin delivery system for orobol.

Keywords: orobol, bentonite, composite, phosphatidylcholine, skin, topical delivery

Introduction

Isoflavones are major phytochemicals in soybeans and are attracting much attention due to their diverse biological activities, including anticancer effects and their protection against osteoporosis and cardiovascular disease.[1–5] In addition to these effects, isoflavones are known to inhibit several signaling pathways of the skin-aging process induced by ultraviolet (UV) light.[6–8] Orobol is one of the major soy isoflavones and is a hydroxylated form of genistein. It was reported that orobol showed a more potent effect than other isoflavones (eg, genistein and daidzein) in suppressing UV-induced metalloproteinase-1 (MMP-1) expression.[6] For example, orobol exhibited an improved skin protection effect by inhibiting MMP-1 expression levels at a concentration of 4 μM in human keratinocyte (HaCaT) and human dermal fibroblast (HDF) cells.[6] However, topical application of orobol has been challenged due to its low water solubility (<50 μg/mL), which in turn hinders absorption through the stratum corneum of the skin and reaching the target dermal layer.[6] Therefore, it is necessary to optimize a suitable formulation for enhancing the topical delivery of orobol, thereby exerting various skin-protective effects against UV-induced photoaging.

Received: 23 September 2022
Accepted: 10 December 2022
Published: 21 December 2022

Bentonite consists of various minerals, including montmorillonite, quartz and zeolite, among which montmorillonite is a major component. It is composed of two tetrahedral sheets with silica and an octahedral sheet with aluminum ions. Interlayer cation exchange leads to a net negative charge and induces unique physical properties in bentonite, including adsorption and swelling.[7] Bentonite has been widely investigated in biomedical fields, mainly in oral drug delivery.[8] It has been formulated as an inactive pharmaceutical excipient for sustaining the release and/or reducing the initial burst release in oral drug delivery systems.[9,10] Although there have been many studies on bentonite as a pharmaceutical excipient for oral delivery, the application of bentonite as a carrier for the topical delivery of active pharmaceutical ingredients (APIs) has rarely been reported. Topical application of bentonite was limited only as an adsorbing excipient for dust, pollen and skin wounds.[11–13] Thus, we investigated the possibility of applying bentonite as a topical delivery carrier for orobol.

It was reported that the main mechanism of adsorption into bentonite is the electrostatic surface interaction between the negatively charged interlayer space of clay sheets and the cationic API. However, the "strong interaction" between API and bentonite has resulted in slow and/or incomplete release of API from the bentonite-API composite.[7,10,14] Thus, it would be necessary to optimize the formulation for enhancing and completing the release of orobol from the complex. Phosphatidylcholine (PC) is amphiphilic in nature and is composed of an esterified glycerol backbone with fatty acids and a choline head.[15,16] Its biocompatible and amphiphilic characteristics have been applied as a solubilizer in diverse pharmaceutical formulations.[16] The hydrophilic choline head group is zwitterionic and consists of a positively charged quaternary amine and a negatively charged phosphate group. Although the charge of PC is neutral as a whole, it is positively charged at pH <3 by the protonation of the phosphate group.[17] Thus, positively charged PC at low pH is suitable for adsorption into the negatively charged interlayer space of bentonite. At the pH of the skin, which ranges from pH 4 ~ pH 6,[18] however, neutralized PC will be easily released from bentonite, which in turn can enhance the solubilization and release of orobol from bentonite. Thus, we hypothesized that entrapping PC as a solubilizer inside the bentonite-orobol composite could be a novel strategy to improve the kinetic release of orobol from the formulation, thereby delivering significantly higher amount of orobol into the skin.

The objective of this study was to investigate the possibility of a bentonite-PC composite formulation for enhancing the topical skin delivery of orobol. The formulation of the orobol-loaded bentonite-PC composite (Bt-PC@Orobol) was optimized based on the results of the adsorbed orobol content and in vitro release studies, followed by in vitro and in vivo hairless mouse skin deposition studies. The physicochemical properties of the composite were characterized by scanning electron microscopy (SEM) and powder X-ray diffraction (pXRD). Then, the toxicity of the optimized composite formulation was further evaluated by blood biochemistry and histological observation of the skin.

Materials and Methods

Preparation of Orobol-Loaded Bentonite Composite Formulations

The adsorption of orobol and PC onto bentonite was conducted by a previous method with minor modification (Figure 1).[9,10,19] Various compositions of orobol-loaded bentonite (Bt@Orobol) and orobol-loaded PC-bentonite (Bt-PC@Orobol) composite formulations prepared in this study are summarized in Table 1. Briefly, to prepare the Bt@Orobol composite formulations, 30 mg of bentonite $(Ca_{0.15}Na_{0.13}K_{0.02})(Ti_{0.02}Al_{1.28}Fe_{0.18}Mg_{0.56})Si_4O_{10}(OH)_2$ (Korea Institute of Geoscience and Mineral Resources, Daejeon, Korea), was dispersed into 24.9 mL of 1 N HCl solution. Separately, different amounts of orobol (3, 6 or 15 mg) (Wuhan Chemfaces Biochemical Co., Ltd., Wuhan, China) were completely dissolved in 5.1 mL of ethanol, after which they were added to the bentonite suspension.[10] The mixture was vortex-mixed at room temperature for 30 min, followed by centrifugation at 2860 × g for 15 min. The sedimented solid fraction was freeze-dried for 24 h. To prepare the Bt-PC@Orobol composite formulations, different amounts of PC (15, 30 or 45 mg) (Phytos, Anyang, Korea) were separately dissolved in 3 mL of ethanol, into which 12 mL of 1 N HCl solution was added. Separately, 30 mg of bentonite was dispersed into 15 mL of 1 N HCl solution. After adding PC solution to the bentonite suspension, they were vortexed for 4 h, followed by centrifugation at 2860 × g for 30 min. After removing the supernatant, the sedimented bentonite-PC composite was collected and freeze-dried for 24 h. Then, orobol (15 mg) dissolved in ethanol (5.1 mL) was added to bentonite-PC composite dispersions in 1 N HCl solution (24.9 mL), followed by vortex mixing and freeze-drying, as described above.

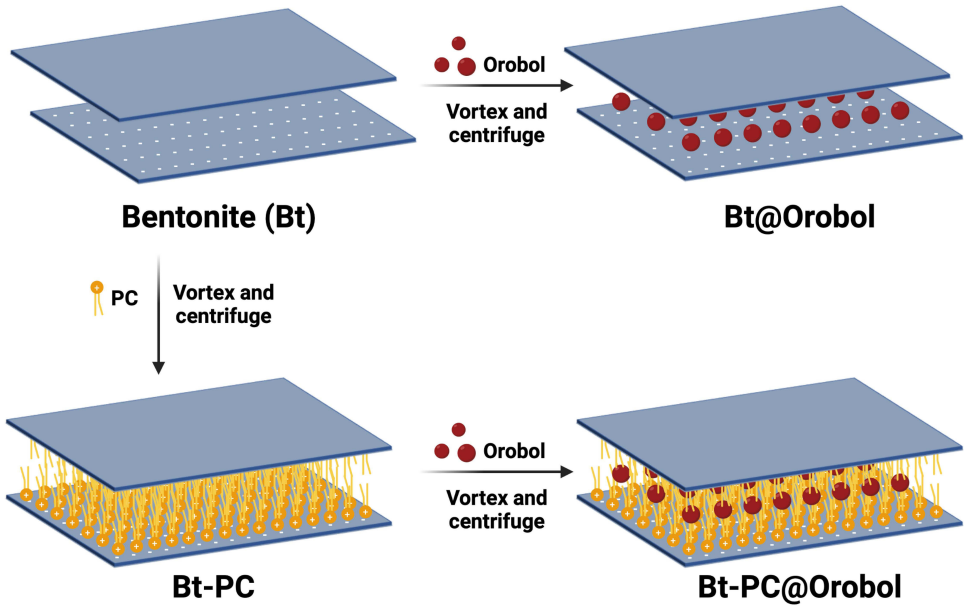

Figure 1 Schematic illustrations of the preparation process of Bt@Orobol and Bt-PC@Orobol composite formulations. Orobol and PC were loaded in the Bt@Orobol and Bt-PC@Orobol formulations based on the adsorption mechanism.[7,10,19]

Determination of the Adsorption Efficiency and Orobol Content in the Composites

The adsorption efficiency and orobol content in bentonite composites were determined as previously reported with slight modification.[9] Briefly, to determine the adsorption efficiency of orobol into bentonite composites during the preparation process, after centrifugation, the supernatant was appropriately diluted and analyzed by using a high-performance liquid chromatography (HPLC) system (Waters, Milford, MA, USA). The mobile phase consisted of 0.2% formic acid in deionized distilled water (DDW) and acetonitrile (60:40, v/v), flowing at 1.0 mL/min. The injection volume of the samples was 20 µL. They were separated by a C_{18} reverse-phase column (Fortis, 250 × 4.6 mm, 5 µm, Cheshire, UK). The eluted mobile phase was monitored with an ultraviolet (UV) detector at 245 nm. The retention time of orobol was 9.3 min. At the lower limit of quantification (LLOQ) of 1.0 µg/mL orobol, the signal-to-noise (S/N) ratio was higher than 5.0. The calibration curve of the standard solution was linear up to 50.0 µg/mL with a correlation coefficient (r^2) of 0.9990.

The orobol contents in Bt@Orobol and Bt-PC@Orobol composites were determined by extracting orobol with methanol. Briefly, an aliquot of each freeze-dried formulation (equivalent to approximately 1 mg of orobol) was dispersed in 1 mL methanol and vortexed for 15 min. After centrifugation at 16,100 × g for 10 min, the supernatant was appropriately diluted with methanol, followed by injection into the HPLC-UV system. The following equations were used to calculate the adsorption efficiency (%) (Equation 1) and the orobol content (%) in bentonite composites (Equation 2):

$$\text{Adsorption efficiency}(\%) = \frac{A_0 - A_S}{A_0} \times 100 \quad (1)$$

Table 1 Orobol Contents and Adsorption Efficiencies of Various Bentonite Composite Formulations

Group	Bt:PC:Orobol (w/w/w)	Orobol Content (%)	Adsorption Efficiency (%)	PC Content (%)
Bt@Orobol (2:1)	2:0:1	35.2 ± 2.3	80.9 ± 3.2	–
Bt@Orobol (5:1)	5:0:1	17.2 ± 0.9	81.6 ± 3.6	–
Bt@Orobol (10:1)	10:0:1	10.3 ± 0.3	81.9 ± 3.4	–
Bt-PC@Orobol (2:1:1)	2:1:1	24.7 ± 0.7	84.2 ± 3.0	13.2 ± 0.4
Bt-PC@Orobol (2:2:1)	2:2:1	22.9 ± 0.7	84.8 ± 1.2	20.8 ± 0.4
Bt-PC@Orobol (2:3:1)	2:3:1	15.7 ± 1.0	79.5 ± 1.9	26.3 ± 1.4

Notes: Data represent the mean ± S.D. (n=3).

$$\text{Orobol content}(\%) = \frac{B_S}{B} \times 100 \quad (2)$$

where A_0 is the initial amount of orobol in the mixture (mg), A_S is the amount of orobol in the supernatant after centrifugation (mg), B_S is the amount of orobol in the bentonite composite (mg), and B is the amount of bentonite composite (mg).

Determination of the Phosphatidylcholine Content

The PC content in bentonite complexes was determined by extracting PC using a mixed solvent of THF and PBS (50:50, v/v) containing 1% (v/v) Tween 20 (Sigma–Aldrich, Saint Louis, MO, USA). Briefly, each composite formulation was dispersed into DDW at 1 mg/mL, followed by diluting 10 times using the extraction solvent. The mixture was vigorously vortexed for 24 h and centrifuged at 16,100 × g for 5 min. The supernatant was collected and then filtered through a 0.2 μm syringe filter. The filtrate was properly diluted with methanol and analyzed by a chromatography-tandem mass spectrometry (LC–MS/MS, Agilent, California, USA) system.[20] The Agilent Technologies 1260 Infinity HPLC system was equipped with an Agilent Technologies 6430 Triple Quad LC–MS system. The mobile phase consisted of 0.2% (v/v) formic acid in DDW and 10 mM ammonium formate in methanol at a 4:96 (v/v) ratio. The flow rate of the mobile phase was 0.4 mL/min, and the injection volume was 5 μL. The samples were separated by a C_8 reverse-phase column (Poroshell 120 2.7 μm EC-C8, 50 × 4.6 mm, Agilent Tech., California, USA) at 40 °C. The electrospray ionization (ESI) process was set with the following parameters: gas temperature 350 °C, gas nebulizing pressure 35 psi, gas flow rate 11 L/min and capillary voltage 4000 V. The mass-to-charge ratio (m/z) of precursor and product ion, fragmentor voltage, collision energy, and cell accelerator voltage of PC were 782.7, 184.3, 214 V, 20 eV and 4 V, respectively. MassHunter Workstation Software Quantitative Analysis (vB.05.00; Agilent Technologies) was used to analyze the LC–MS/MS data. The retention time of PC was 4 min. The standard solutions for the calibration curve were prepared by serial dilution of a stock solution (10 mg/mL of PC in DMSO) with methanol. At the LLOQ of 10 ng/mL, the S/N ratio of the PC peak was 30.5. The calibration curve of the standard solution was linear up to 1000 ng/mL. The following equation was used to calculate the PC content (%) in bentonite composites (Equation 3):

$$\text{PC content}(\%) = \frac{C_{CP}}{C} \times 100 \quad (3)$$

where C_{CP} is the amount of PC measured from HPLC/MS-MS analysis (mg) and C is the amount of bentonite composite (mg).

In vitro Release Study of Orobol from the Bentonite Composite Formulations

The in vitro release of orobol from the Bt@Orobol and Bt-PC@Orobol composites was performed using the dialysis membrane method, following previous reports with slight modification.[21,22] Briefly, an aliquot (equivalent to 1 mg as orobol) of each composite or orobol powder was dispersed in 3 mL of DDW and put into a dialysis bag (MW cut off: 12,000–14,000 Da, Viskase, Illinois, USA), which was then immersed into 27 mL of release medium in a 50 mL conical tube.[23] Phosphate buffered saline (PBS, Corning, Virginia, USA) (pH 5.5) containing 0.5% (w/v) of SDS was chosen as the release medium. These tubes were shaken horizontally at a speed of 50 rpm at 32 °C for 12 h. An aliquot (0.3 mL) of release medium was collected at 0.25, 0.5, 1, 2, 4, 6, 8, and 12 h, and then an equal volume of fresh medium was replenished to maintain a constant volume. The concentration of orobol in the release medium was determined following the HPLC-UV method described above.

The cumulative amount of orobol released (F; %) against time (t) profile was fitted to the following mathematical models (Equations 4–7) using the DDSolver program:[10,24–26]

$$\text{First} - \text{order model}: \ F = F_{max} \times \left(1 - e^{-kt}\right) \quad (4)$$

$$\text{Higuchi model}: \ F = k_H \times t^{0.5} \quad (5)$$

$$\text{Korsmeyer} - \text{Peppas model}: \ F = k_{KP} \times t^{n} \quad (6)$$

$$\text{Hixson} - \text{Crowell model}: \ F = 100 \times \left[1 - (1 - k_{HC} \times t)^3\right] \quad (7)$$

where F_{max} is the maximum cumulative amount of orobol released, whereas k, k_H, k_{KP} and k_{HC} are the release rate constants of each model.

Skin Deposition Study in Hairless Mice

The in vitro and in vivo skin deposition of orobol after applying various compositions of orobol-loaded bentonite composite formulations was investigated by a method described in the literature with slight modification.[23] The animal study protocol was approved by Seoul National University Institutional Animal Care and Use Committee (IACUC) (No. SNU-170103-10), which followed the American Veterinary Medical Association (AVMA) Guidelines for the Euthanasia of Animals: 2020 Edition and the Guide for the Care and Use of Laboratory Animals (Eighth Edition).

In vitro Skin Deposition Study

The in vitro hairless mouse skin deposition of orobol was evaluated by using Keshary–Chien diffusion cells (surface area of 1.77 cm^2) at 32 °C. SKH1 hairless mice (Orient Bio Inc., Sung-nam, Republic of Korea) were sacrificed by cervical dislocation, and the excised dorsal skin was placed between the donor and receptor cells. The receptor part of the diffusion cells was filled with PBS (pH 7.4) containing SDS (0.5%, w/v) and stirred with a magnetic bar at 600 rpm. Orobol aqueous suspension (as the control) or various orobol-loaded bentonite composite formulations (equivalent to 1.0 mg of orobol) in DDW were applied to the donor cells, which were then sealed with parafilm to avoid evaporation. After applying the samples for 24 h, the skin was removed from the diffusion cells and washed three times with methanol. The amounts of orobol in the stratum corneum (SC) and epidermis/dermis layers were separately determined by a previous method with slight modification.[23] Briefly, polyester adhesive tape (CuDerm Co., Texas, USA) was applied five times to the SC part of the skin. These tapes were then collected into a 2.0 mL Eppendorf tube. The remaining skin samples were chopped with scissors and ground into fine powder by using a mortar and pestle in the presence of liquid nitrogen. The skin powder was then collected into a 2.0 mL Eppendorf tube by using cellophane adhesive tape. After collecting the samples, methanol (1 mL) was added to extract the orobol. These tubes were shaken for 3 h and centrifuged for 5 min at 16,000 × g. The supernatant was diluted with methanol and analyzed by an LC–MS/MS system (Agilent, California, USA) equipped with an Agilent Technologies 6430 Triple Quad LC–MS system. The samples were separated by an Accucore RP-MS C_{18} column (2.6 μm, 50 mm × 3 mm; Thermo Scientific, Lithuania) at 40 °C. The mobile phase consisted of 0.2% formic acid in DDW and acetonitrile at a ratio of 45:55 (v/v). The injection volume of the sample and the flow rate of the mobile phase were 5 μL and 0.4 mL/mL, respectively. The ESI process was set with the following parameters: gas temperature 350 °C, gas nebulizing pressure 15 psi, gas flow rate 11 L/min and capillary voltage 4000 V. The m/z of precursor and product ion, fragmentor voltage, collision energy, and cell accelerator voltage of orobol were 287.2, 153.0, 165 V, 30 eV and 4 V, respectively. The retention time of orobol was 0.9 min. The calibration curve was obtained from the standard solutions prepared by serial dilution of a stock solution (10.0 mg/mL orobol in DMSO) with methanol, which was linear in the concentration range of 10.0–1000 ng/mL with a correlation coefficient (r^2) of 0.998. At the LLOQ of 10 ng/mL, the S/N ratio of the orobol peak was higher than 5.0.

In vivo Skin Deposition Study

The in vivo skin deposition of orobol was evaluated using male SKH1 hairless mice. After lightly anesthetizing the mice by intramuscular injection of Zoletil® 50 at 50 mg/kg, they were fixed with the dorsal side facing upward. Then, the donor patch of Keshary–Chien diffusion cells (area of 1.77 cm^2) was fixed on the dorsal skin using surgical glue (Vet Bond, 3 M Co., St. Paul, MN, USA). After recovering from the anesthesia, an aliquot (0.35 mL) of orobol aqueous suspension (as the control) or the Bt-PC@Orobol (2:2:1) composite formulation in DDW was applied into the chamber at a dose of 50 mg/kg orobol. After applying the formulation for 2 h or 6 h, the hairless mice were sacrificed by cervical dislocation. Then, the skin of the diffusion area was removed and pretreated to analyze the concentration of orobol using the LC–MS system, as described above.

Characterization of Bentonite Composite Formulations

The surface morphologies of bentonite, orobol, PC, Bt@Orobol (2:1), Bt-PC and Bt-PC@Orobol (2:2:1) were observed by field emission scanning electron microscopy (FE-SEM, SUPRA 55VP, Carl Zeiss, Germany). Each sample was layered on a copper tape and then coated with platinum for 150 sec. The plasma current and accelerating voltage for the coating were 30 mA plasma and 2.0 kV, respectively.

Powder X-ray diffraction analyses (pXRD) of PC, Bt, orobol, bentonite composite formulations and their physical mixtures were conducted. D8 ADVANCE with DAVINCI (BRUKER, Germany) was used with CuKα1 radiation (λ = 1.5418 Å) generated under 40 kV and 40 mA conditions. Each sample was scanned between 3 and 45 degrees in the 2θ range with a 0.02-degree step angle at a 0.5 sec/step scan speed. The intensity of the pXRD peaks was normalized after detection.

In vitro Cytotoxicity Study

The in vitro cytotoxicities of orobol, Bt-PC and Bt-PC@Orobol (2:2:1) composite formulation were evaluated in human keratinocyte (HaCaT) cells (Thermo Fisher Scientific, Massachusetts, USA). Briefly, cells were seeded on 96-well plates at 1.0×10^4 cells/100 μL in complete Dulbecco's modified Eagle's medium supplemented with 10% fetal bovine serum and 0.5% penicillin–streptomycin. After applying various concentrations of orobol solution ($3 \times 10^{-4} \sim 3 \times 10^1$ μg/mL) or bentonite composite formulation (Bt-PC or Bt-PC@Orobol) at $1 \times 10^{-3} \sim 3 \times 10^2$ μg/mL, the cells were incubated for 24 h or 48 h at 37 °C. Then, the cytotoxicity was assessed by a 3-(4,5-dimethylthiazol-2-yl)-5(3-carboxymethoxyphenyl)-2-(4-sulfophenyl)-2H-tetrazolium (MTS) assay (CellTiter 96 Aqueous One Solution Cell Proliferation Assay, Promega, Milan, Italy) according to the manufacturer's instructions. The absorbance was read in a microplate reader (Multiskan Microplate Spectrophotometer; Thermo Fisher Scientific, Massachusetts, USA) at 492 nm.

In vivo Toxicity Study in Mice

The in vivo toxicity of the Bt-PC@Orobol (2:2:1) composite formulation was evaluated by blood biochemistry and histological observation of the skin after 24 h of topical application on SKH1 hairless mice (approximately 20 g).[27,28] Briefly, after fixing the mice following the protocol described above for the in vivo skin deposition study, 0.35 mL of orobol aqueous suspension or Bt-PC@Orobol (2:2:1) composite formulation in DDW (50 mg/kg as orobol) was applied to the back of each mouse. After 24 h of application, the mice were sacrificed by blood collection through cardiac puncture, and the whole skin was dissected. The serum was separated by standing blood samples for 1 h at room temperature, after which they were centrifuged at 16,000 × g for 10 min. The levels of alanine transaminase (GPT), serum creatinine (CRE), blood urea nitrogen (BUN), serum albumin (ALB) and total protein (TP) were analyzed using a Fuji Dri-Chem 3500s (Fujifilm Corp., Tokyo, Japan). Excised skin samples were fixed in a 10% neutral buffered formalin solution (Sigma Aldrich). After deparaffinizing the cross-sectioned skin tissue slices, they were hydrated with a series of ethanol solutions. Each specimen was then stained with hematoxylin and eosin (H&E) reagent and Masson's trichrome staining. The microscopy images were observed using an Olympus IX70 (Olympus Co., Tokyo. Japan). All results were compared with those of untreated mice.

Statistical Analysis

All experiments were performed at least three times, and the acquired data are presented as the mean ± standard deviation (S. D.). Statistical analysis was performed using Student's *t*-test or one-way analysis of variance (ANOVA) followed by Tukey's post hoc multiple comparison test (GraphPad Prism version 9.0.2, California, U.S.). A p value <0.05 was considered statistically significant.

Results and Discussion

Preparation of Orobol-Loaded Bentonite Complex Formulations

Table 1 shows the orobol contents and the orobol adsorption efficiencies when orobol-loaded bentonite composite formulations (Bt@Orobol) were prepared by varying the weight ratio of bentonite to orobol. As the weight ratio of bentonite increased from 2:1 to 10:1, the orobol content linearly decreased from 35.2% to 10.3%, while the orobol adsorption efficiencies remained constant at approximately 81%. These results indicate that the adsorption of orobol onto

bentonite was not saturated up to a 2:1 weight ratio. Since the orobol content was highest at a 2:1 weight ratio, it was chosen for further optimization of bentonite composites with PC.

To prepare the Bt-PC@Orobol composite formulations with the weight ratios shown in Table 1, bentonite-PC composites with various weight ratios of bentonite to PC (2:1, 2:2 and 2:3) were first prepared, followed by loading orobol at a 2:1 weight ratio of bentonite to orobol. The PC content (%) proportionally increased from 13.2% to 26.3% as the input amount of PC increased from a 2:1 to 2:3 ratio of bentonite to PC. However, the adsorption efficiency of orobol in the Bt-PC@Orobol (2:3:1) composite formulation significantly decreased up to 79.5%, while those in the Bt-PC@Orobol (2:1:1) and Bt-PC@Orobol (2:2:1) composites did not change, remaining at approximately 84%. These results implied that the adsorption of orobol and PC on bentonite could have competed at high PC contents, resulting in a significant decrease in the orobol content and the adsorption efficiency.

The mechanism of drug loading into the bentonite composite includes pH-dependent cation exchange and physical adsorption.[10] During the preparation of bentonite-drug complex, pH of the medium plays a very important role since acidic solution keeps cationic molecules in their protonated form, which in turn enhances the exchange with intercalated cations and electrostatic surface interaction with negatively charged interlayer space of clay sheets.[8,10] Thus, orobol-loaded bentonite composites were prepared in acidic aqueous HCl solution to enhance the adsorption efficiency. It is interesting to note that since PC is also positively charged at pH <3, adsorption of orobol and PC could have competed at high PC content. Thus, it is necessary to optimize the PC content to maximize the adsorption efficiency of orobol in the composites.

In vitro Release of Orobol from Bentonite Complexes

Figure 2 shows the in vitro release profiles of orobol from bentonite-orobol complex formulations with various compositions. The pH of the release medium was 5.5 to mimic the average pH of normal adult skin, and 0.5% (w/v) SDS was added to the release medium to maintain the sink condition. The extent of orobol released from the bentonite composite formulations was significantly enhanced compared to the orobol suspension. Moreover, the release of orobol from Bt-PC@Orobol (2:1:1) and Bt-PC@Orobol (2:2:1) was further enhanced (up to 80% at 12 h) compared to that from Bt@Orobol (2:1) (up to 60% at 12 h), indicating that PC could be an effective solubilizer for increasing the dissolution of orobol from the bentonite composite formulation. However, it is notable that the release of orobol from Bt-PC@Orobol (2:3:1) decreased compared to the other Bt-PC@Orobol composite formulations. These data suggest that the adsorption of orobol into the interlayer of bentonite enhanced the dissolution of orobol. Moreover, the addition of an optimum amount of PC to the composite formulation further enhanced the dissolution of orobol. However, an excess amount of PC could hinder the release of orobol from the bentonite composite due to the hydrophobicity of PC.

The in vitro release profiles of orobol were fitted to the four mathematical release kinetic models, including the first-order, Higuchi, Korsmeyer-Peppas and Hixson-Crowell models, to understand the release mechanism(s) of orobol from

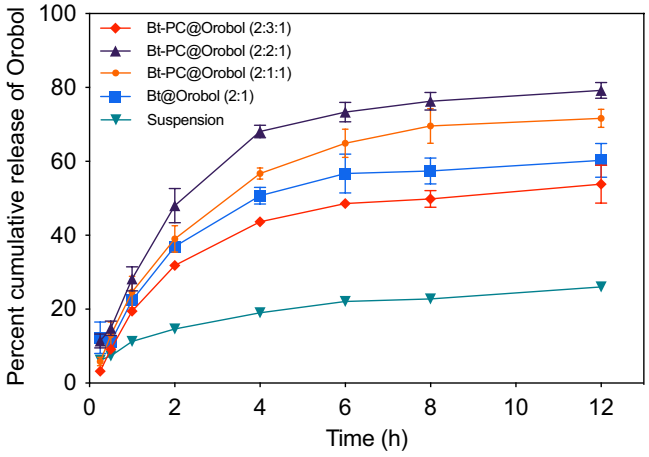

Figure 2 In vitro release profiles of orobol from the bentonite-orobol composites into PBS medium (pH 5.5) containing 0.5% (w/v) SDS.
Notes: Orobol suspension was the control for comparison. Data represent the mean ± S.D. (n = 3).

the bentonite composite formulations. The fitting results revealed that there was a difference in release mechanism between orobol suspension group and orobol-bentonite composite formulations (Table 2). The release kinetic of orobol from the suspension exhibited the highest correlation coefficient when fitted with the Korsmeyer-Peppas model, implying that Fickian diffusion was the main release mechanism. On the hand, the first-order model exhibited the highest coefficients of determination in all orobol bentonite composite formulations, indicating that the release of orobol was highly dependent on the amount of orobol loaded on the composites. These results were consistent with the previous report that the release of orobol from the bentonite composites follows the first-order release kinetic model.[10]

Skin Deposition of Orobol in Hairless Mice

Figure 3A shows the in vitro deposition of orobol in the stratum corneum and epidermis/dermis of hairless mouse skin at 24 h after topical administration of orobol suspension or bentonite composite formulations at 1.0 mg per diffusion cell as orobol. Hairless mouse skin has been extensively applied as an alternative to human skin due to their similarity in composition and good correlation in absorption profiles.[23,29,30] Compared to the suspension group, the in vitro skin deposition of orobol was higher in the bentonite composite groups. These results were consistent with those of the in vitro release study (Figure 2), indicating that enhanced dissolution of orobol by bentonite composite formulations could have contributed to the increased skin absorption. Moreover, the addition of PC to the formulations further enhanced the skin deposition of orobol. Notably, the Bt-PC@Orobol (2:2:1) group showed higher skin deposition of orobol than the Bt-PC@Orobol (2:1:1) group, yet the Bt-PC@Orobol (2:3:1) group showed a reduction in skin deposition. Thus, PC in the bentonite composite not only enhanced the dissolution of orobol as a solubilizer but also increased skin absorption as a permeation enhancer.[31–33] However, a high content of hydrophobic PC in the composite formulations could hinder the release of orobol onto the skin, which in turn decreased the skin absorption of orobol. The highest deposition of orobol into both the stratum corneum and dermis/epidermis was observed in the Bt-PC@Orobol (2:2:1) group, which was approximately 2.4-fold higher than that from the suspension group ($p < 0.01$). Based on these results, Bt-PC@Orobol (2:2:1) was selected as an optimum composite formulation of orobol for further evaluation.

Figure 3B shows the in vivo deposition of orobol in the stratum corneum and epidermis/dermis of hairless mouse skin at 2 h and 6 h after topical application of orobol suspension or orobol-loaded Bt-PC@Orobol (2:2:1) bentonite composite formulation at a dose of 50 mg/kg as orobol. The total amount of orobol deposited in the skin was significantly higher in the Bt-PC@Orobol (2:2:1) formulation group than in the suspension formulation at both 2 h ($p < 0.05$) and 6 h ($p < 0.01$). The results of the in vitro release study and the in vitro/in vivo skin deposition study consistently support that the adsorption of orobol into bentonite enhanced the dissolution of orobol, which in turn increased the skin absorption. The addition of PC to the bentonite composite synergistically enhanced the dissolution and skin absorption of orobol, thereby increasing its skin deposition.

Characterization of Bentonite Complex Formulations

To understand the underlying mechanism(s) of the enhanced dissolution and skin deposition of orobol by bentonite composite formulations, surface morphology and pXRD studies were conducted. Figure 4A shows the surface morphologies of the bentonite composite and each excipient observed by FE-SEM. Bentonite showed a porous bulky powder structure, whereas a polyhedron crystalline powder form was observed in orobol. A typical lipid-like smooth surface

Table 2 Mathematical Kinetic Modeling on Orobol Release Profiles (Refer to Figure 2)

Model	First-Order			Higuchi		Korsmeyer-Peppas			Hixson-Crowell	
	R^2	k	F_{max}	R^2	k_H	R^2	k_{KP}	n	R^2	k_{HC}
Suspension	0.932	0.58	23.5	0.891	8.50	0.985	11.046	0.358	0.156	0.011
Bt@Orobol (2:1)	0.984	0.49	59.7	0.879	20.75	0.920	25.125	0.396	0.564	0.036
Bt-PC@Orobol (2:1:1)	0.996	0.41	72.4	0.922	23.98	0.935	26.271	0.452	0.791	0.047
Bt-PC@Orobol (2:2:1)	0.996	0.47	79.2	0.900	27.21	0.918	31.913	0.415	0.811	0.068
Bt-PC@Orobol (2:3:1)	0.994	0.44	53.1	0.902	17.96	0.917	20.08	0.440	0.641	0.028

Notes: The coefficient of determination is presented as R^2. F_{max} is the maximum cumulative release. Release rate constants of corresponding models are expressed as k, k_H, k_{KP} k_{HC}.

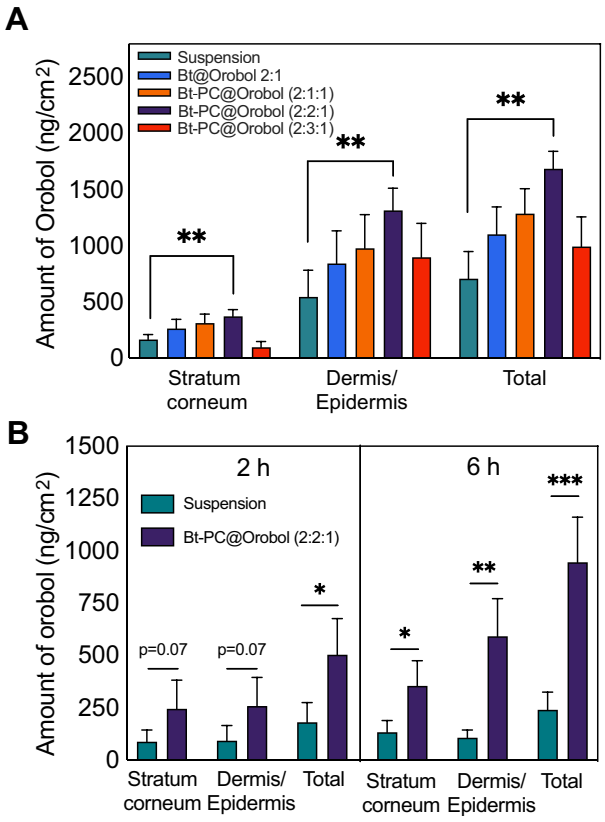

Figure 3 (**A**) In vitro deposition of orobol in the stratum corneum and epidermis/dermis of hairless mouse skin at 24 h after topical administration of orobol suspension or bentonite composite formulation at 1.0 mg per diffusion cell as orobol. (**B**) In vivo deposition of orobol in the stratum corneum and epidermis/dermis of hairless mouse skin at 2 h and 6 h after topical application of orobol suspension or orobol-loaded Bt-PC@Orobol (2:2:1) bentonite composite formulation at a dose of 50 mg/kg as orobol.
Notes: *p < 0.05, **p < 0.01, and ***p < 0.001. Data represent the mean ± S.D. (n = 3).

morphology was observed in PC without a crystalline structure. It is notable that the surface morphologies of all composite formulations, including Bt@Orobol (2:1), Bt-PC and Bt-PC@Orobol (2:2:1), were similar to that of bentonite powder. The disappearance of the smooth morphology of PC and the crystalline structure of orobol supports that PC and orobol intercalated into the interlayer of the BT structure. Moreover, the disappearance of the polyhedron-like crystal structure of orobol implies that orobol could be adsorbed into bentonite composite formulations in an amorphous state.

Thus, pXRD analysis was performed to investigate the crystalline state of orobol in the composite formulations, which was then compared with that in the physical mixture of the excipients of the composite formulations. As shown in Figure 4B, PC showed a broad peak at approximately 20 degrees without distinct crystalline peaks, while orobol and bentonite showed distinct crystalline peaks between 5 and 40 degrees, which were comparable with previous reports.[6,9,34] However, the crystalline peaks of orobol disappeared in bentonite composite formulations of Bt@Orobol (2:1) and Bt-PC@Orobol (2:2:1), and they were similar to those of bentonite. Since the physical mixture of excipients showed the crystalline peaks of orobol, these pXRD observations indicate that orobol was absorbed into the bentonite interlayer in an amorphous state in the composite formulations. These results were consistent with our previous reports that the adsorption of API into bentonite in amorphous form enhanced the release of API in comparison with its corresponding crystalline form.[6,9,34] Thus, the enhanced dissolution of orobol compared to the orobol suspension (Figure 2) could be due to the formation of amorphous orobol in the bentonite composite formulations, which in turn increased the driving force of diffusion and deposition into the skin (Figure 3). Additionally, the addition of an optimum amount of PC in the bentonite-orobol composite formulation further enhanced the solubilization of orobol, thereby increasing the skin deposition of orobol. As previously reported, the vesicle-to-micelle transition of PC in an aqueous environment seems to facilitate the release and diffusion of orobol into the skin.[30] Thus, the addition of PC to the bentonite-orobol composite could be a useful strategy for not only improving the incomplete release of orobol from the composite formulations but also increasing skin deposition by enhancing the solubilization and diffusion of orobol.

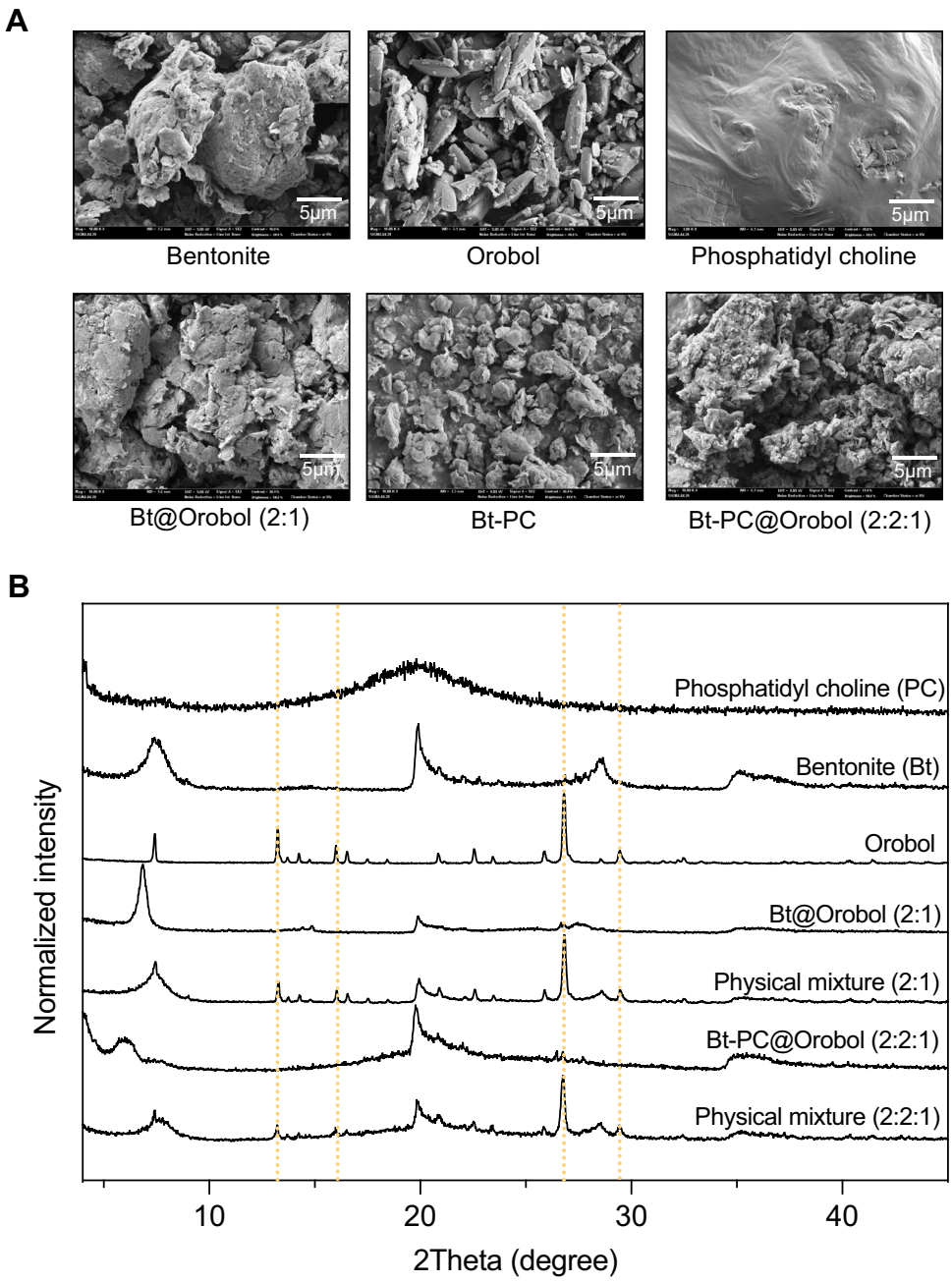

Figure 4 Physicochemical characterization of orobol-loaded bentonite composite formulations. (**A**) FE-SEM images of bentonite, orobol, phosphatidylcholine and bentonite composite formulations. The scale bar is 5 μm. (**B**) pXRD of PC, bentonite, orobol, bentonite composite formulations and physical mixtures.

Toxicity Studies

Figure 5A shows the in vitro cytotoxicities of orobol, Bt-PC and the Bt-PC@Orobol (2:2:1) composite formulation against HaCaT cells. When the cytotoxicity was determined using the MTS-based assay after applying orobol solution for 24 h or 48 h, higher than 95% cell viability was observed within the concentration range tested ($3 \times 10^{-4} \sim 3 \times 10^{1}$ μg/mL), implying negligible cytotoxicity of orobol against HaCaT cells. Neither the Bt-PC nor the Bt-PC@Orobol (2:2:1) composite formulations showed significant cytotoxicity after applying up to 300 μg/mL, indicating the nontoxic and biocompatible nature of bentonite and PC at the cellular level. In previous studies, no cytotoxic effect of bentonite was reported after applying up to 125 μg/mL bentonite to human colorectal adenocarcinoma cells (Caco-2).[35,36] Moreover, since the stratum corneum layer of the skin acts as a formidable protective barrier, it is unlikely that bentonite composite formulations would show a significant cytotoxic effect on the dermis/epidermis after topical skin application.

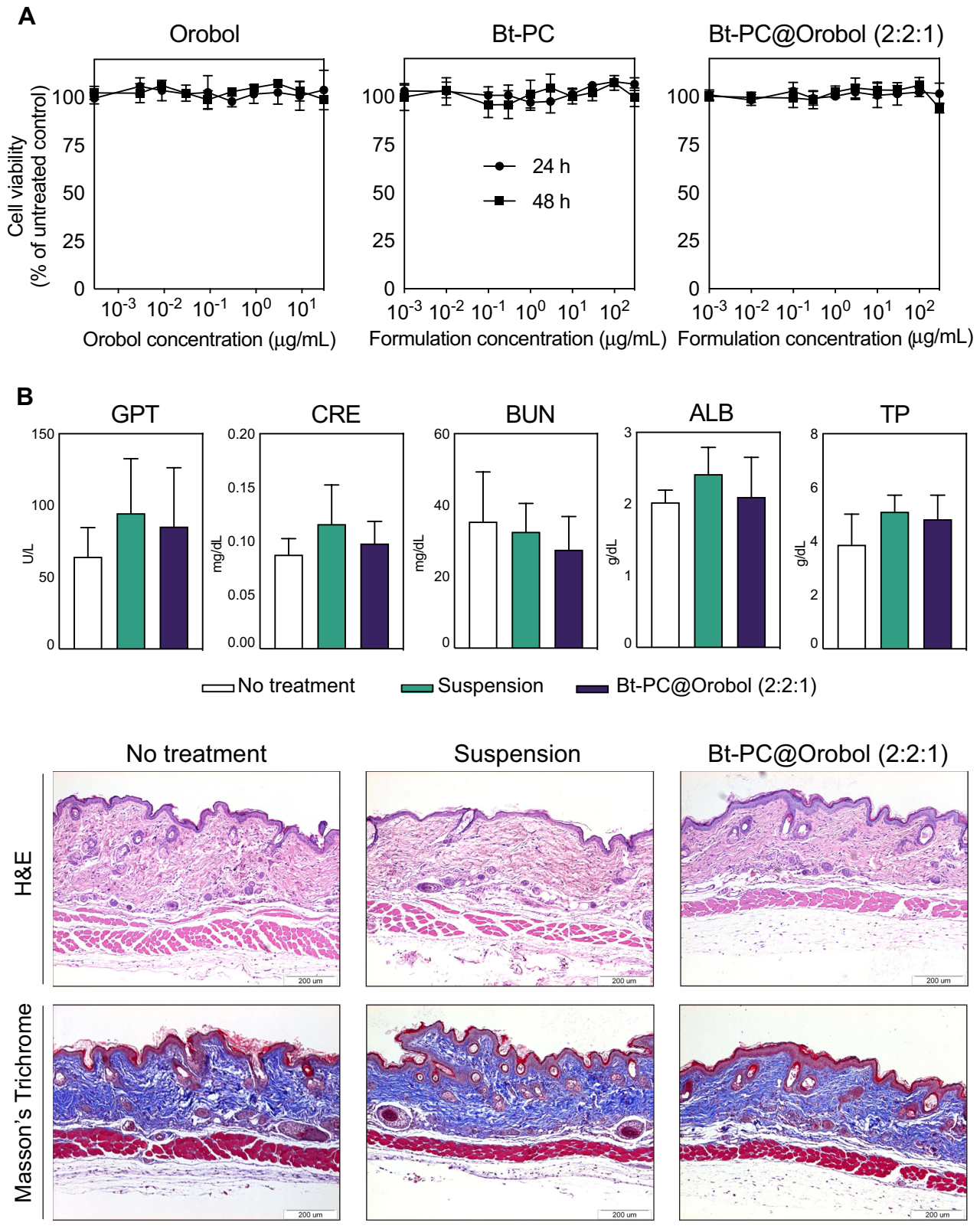

Figure 5 (**A**) In vitro cytotoxicity of orobol, Bt-PC and Bt-PC@Orobol (2:2:1) in human keratinocyte HaCaT cells determined by MTS-based assay after 24 h or 48 h of application. (**B**) In vivo toxicity of Bt-PC@Orobol (2:2:1) and orobol aqueous suspension in hairless mice after 24 h of topical application at a dose of 50 mg/kg as orobol. The blood chemistry test results and histopathological observations (H&E and Masson's trichrome staining, x10) were compared with those of untreated mice.
Notes: Data represent the mean ± S.D. (n = 3). The scale bar is 200 μm.

Figure 5B shows the histological observations of hairless mouse skin after topical application of orobol suspension or Bt-PC@Orobol (2:2:1) composite formulation for 24 h at a dose of 50 mg/kg orobol. There were no significant differences in the results of the blood chemistry tests, including the levels of serum GPT, CRE, ALB and TP, among the groups ($p > 0.05$). Moreover, no significant difference was noted in either group compared to the untreated control group after H&E and Masson's trichrome staining of the skin. PC and bentonite are known to be nonirritating components for topical application.[37,38] Orobol was also reported to have negligible skin irritation in a human study.[6] Thus, these findings from in vitro and in vivo toxicity studies support the safety of the bentonite complex formulation for topical skin delivery.

Conclusion

The formulation of the bentonite-PC composite was optimized to enhance the topical skin delivery of orobol. The optimized composite formulation demonstrated the enhanced dissolution and skin deposition of orobol. Moreover, the addition of PC to the formulation not only improved the dissolution and incomplete release of orobol from the bentonite composite but also enhanced the deposition of orobol in the skin. The SEM and pXRD studies supported that orobol was adsorbed onto BT in an amorphous state, which in turn enhanced the dissolution of orobol. No significant toxicity of the optimized bentonite composite formulation was observed in the histological observation and blood chemistry studies. Thus, entrapping PC inside the bentonite-orobol composite could be a useful strategy to enhance the topical skin delivery of orobol by improving the kinetic release from the formulation. Taken together, the orobol-loaded bentonite-PC composite formulation could be a potential platform for the topical skin delivery of orobol. Further translational research needs to be conducted to develop the orobol-bentonite composite into various pharmaceutical dosage forms (ie, cream, liniment and hydrogel) for clinical application.

Acknowledgments

This work was supported by a Seoul National University Research Grant in 2020 (370C-20200095) and National Research Foundation of Korea (NRF) grants funded by the Ministry of Science and ICT (Nos. NRF-2018R1A5A2024425, NRF-2018M3A7B4071203 and NRF-2020R1A2C2099983).

Disclosure

The authors declare that they have no competing financial interests or personal relationships that could have influenced the work reported in this paper.

References

1. Wei P, Liu M, Chen Y, Chen DC. Systematic review of soy isoflavone supplements on osteoporosis in women. *Asian Pac J Trop Med*. 2012;5(3):243–248. doi:10.1016/S1995-7645(12)60033-9
2. Zheng X, Lee SK, Chun OK. Soy isoflavones osteoporotic bone loss: a review with an emphasis on modulation of bone remodeling. *J Med Food*. 2016;19(1):1–14. doi:10.1089/jmf.2015.0045
3. Abshirini M, Omidian M, Kord-Varkaneh H. Effect of soy protein containing isoflavones on endothelial and vascular function in postmenopausal women: a systematic review and meta-analysis of randomized controlled trials. *Menopause*. 2020;27(12):1425–1433. doi:10.1097/GME.0000000000001622
4. Rimbach G, Boesch-Saadatmandi C, Frank J, et al. Dietary isoflavones in the prevention of cardiovascular disease - A molecular perspective. *Food Chem Toxicol*. 2008;46(4):1308–1319. doi:10.1016/j.fct.2007.06.029
5. Yamagata K. Soy isoflavones inhibit endothelial cell dysfunction and prevent cardiovascular disease. *J Cardiovasc Pharmacol*. 2019;74(3):201–209. doi:10.1097/FJC.0000000000000708
6. Kim MH, Jeon YE, Kang S, et al. Lipid nanoparticles for enhancing the physicochemical stability and topical skin delivery of orobol. *Pharmaceutics*. 2020;12(9):1–16. doi:10.3390/pharmaceutics12090845
7. Park JH, Shin HJ, Kim MH, et al. Application of montmorillonite in bentonite as a pharmaceutical excipient in drug delivery systems. *J Pharm Investig*. 2016;46(4):363–375. doi:10.1007/s40005-016-0258-8
8. Iannuccelli V, Maretti E, Bellini A, et al. Organo-modified bentonite for gentamicin topical application: interlayer structure and in vivo skin permeation. *Appl Clay Sci*. 2018;158:158–168. doi:10.1016/j.clay.2018.03.029
9. Jung SY, Park JH, Baek MJ, et al. Development of an oral bentonite-based modified-release freeze-dried powder of vactosertib: pharmacokinetics and anti-colitis activity in rodent models of ulcerative colitis. *Int J Pharm*. 2020;578:119103. doi:10.1016/j.ijpharm.2020.119103
10. Baek MJ, Shin HJ, Park JH, et al. Preparation and evaluation of the doxazosin-bentonite composite as a pH-dependent controlled-release oral formulation. *Appl Clay Sci*. 2022;229:106677. doi:10.1016/J.CLAY.2022.106677
11. Askari M, Afshar M, Naghizadeh A, Khorashadizadeh M, Zardast M. Bentonite nanoparticles and honey co-administration effects on skin wound healing: experimental study in the BALB/c MICE. *Int J Lower Extremity Wounds*. 2022;153473462211184. doi:10.1177/15347346221118497

12. Nozari M, Gholizadeh M, Zahiri Oghani F, Tahvildari K. Studies on novel chitosan/alginate and chitosan/bentonite flexible films incorporated with ZnO nano particles for accelerating dermal burn healing: in vivo and in vitro evaluation. *Int J Biol Macromol*. 2021;184:235–249. doi:10.1016/j.ijbiomac.2021.06.066
13. Iwanaga T, Nioh A, Reed N, Kiyokawa H, Akatsuka H. A novel water-in-oil emulsion with a lecithin-modified bentonite prevents skin damage from urban dust and cedar pollen. *Int J Cosmet Sci*. 2020;42(3):229–236. doi:10.1111/ics.12605
14. Dziadkowiec J, Mansa R, Quintela A, Rocha F, Detellier C. Preparation, characterization and application in controlled release of Ibuprofen-loaded Guar Gum/Montmorillonite Bionanocomposites. *Appl Clay Sci*. 2017;135:52–63. doi:10.1016/j.clay.2016.09.003
15. Gautschi N, van Hoogevest P, Kuentz M. Molecular insights into the formation of drug-monoacyl phosphatidylcholine solid dispersions for oral delivery. *Eur J Pharma Sci*. 2017;108:93–100. doi:10.1016/j.ejps.2016.05.023
16. van Hoogevest P. Review – an update on the use of oral phospholipid excipients. *Eur J Pharma Sci*. 2017;108:1–12. doi:10.1016/j.ejps.2017.07.008
17. Boggs JM. Lipid intermolecular hydrogen bonding: influence on structural organization and membrane function. *BBA*. 1987;906(3):353–404. doi:10.1016/0304-4157(87)90017-7
18. Lukić M, Pantelić I, Savić SD. Towards optimal pH of the skin and topical formulations: from the current state of the art to tailored products. *Cosmetics*. 2021;8(3). doi:10.3390/cosmetics8030069
19. Baek MJ, Kim GH, Park JH, et al. Effect of phosphatidylcholine in bentonite-quetiapine complex on enhancing drug release and oral bioavailability. *Int J Pharm*. 2022;628:122347. doi:10.1016/J.IJPHARM.2022.122347
20. Walczak J, Bocian S, Buszewski B. Two-dimensional high performance liquid chromatography-mass spectrometry for phosphatidylcholine analysis in egg yolk. *Food Anal Methods*. 2015;8(3):661–667. doi:10.1007/s12161-014-9942-3
21. Kim MH, Park JH, Nguyen DT, et al. Hyaluronidase inhibitor-incorporated cross-linked hyaluronic acid hydrogels for subcutaneous injection. *Pharmaceutics*. 2021;13(2):1–16. doi:10.3390/pharmaceutics13020170
22. Lee SY, Park JH, Yang M, et al. Ferrous sulfate-directed dual-cross-linked hyaluronic acid hydrogels with long-term delivery of donepezil. *Int J Pharm*. 2020;582. doi:10.1016/j.ijpharm.2020.119309
23. Kim KT, Kim MH, Park JH, et al. Microemulsion-based hydrogels for enhancing epidermal/dermal deposition of topically administered 20 (S)-protopanaxadiol: in vitro and in vivo evaluation studies. *J Ginseng Res*. 2018;42(4):512–523. doi:10.1016/j.jgr.2017.07.005
24. Zhang Y, Huo M, Zhou J, et al. DDSolver: an add-in program for modeling and comparison of drug dissolution profiles. *AAPS J*. 2010;12(3):263–271. doi:10.1208/s12248-010-9185-1
25. Kang NW, Lee JY, Kim DD. Hydroxyapatite-binding albumin nanoclusters for enhancing bone tumor chemotherapy. *J Control Release*. 2022;342:111–121. doi:10.1016/j.jconrel.2021.12.039
26. Costa P, Sousa Lobo J M . Modeling and comparison of dissolution profiles. *Eur J Pharma Sci*. 2001;13:123–133. doi:10.1016/S0928-0987(01)00095-1
27. Back PI, Balestrin LA, Fachel FNS, et al. Hydrogels containing soybean isoflavone aglycones-rich fraction-loaded nanoemulsions for wound healing treatment – in vitro and in vivo studies. *Colloids Surf B Biointerfaces*. 2020;196:111301. doi:10.1016/j.colsurfb.2020.111301
28. Munro IC, Harwood M, Hlywka JJ, et al. Lead review article soy isoo avones: a safety review. *Nutr Rev*. 2003;61:1–33.
29. Kim KT, Kim JS, Kim MH, et al. Effect of enhancers on in vitro and in vivo skin permeation and deposition of S-methyl-L-methionine. *Biomol Ther*. 2017;25(4):434–440. doi:10.4062/biomolther.2016.254
30. Jung E, Kang YP, Yoon IS, et al. Effect of permeation enhancers on transdermal delivery of fluoxetine: in vitro and in vivo evaluation. *Int J Pharm*. 2013;456(2):362–369. doi:10.1016/j.ijpharm.2013.08.080
31. Li Y, Xu F, Li X, et al. Development of curcumin-loaded composite phospholipid ethosomes for enhanced skin permeability and vesicle stability. *Int J Pharm*. 2021;592:119936. doi:10.1016/j.ijpharm.2020.119936
32. Spernath A, Aserin A, Sintov AC, Garti N. Phosphatidylcholine embedded micellar systems: enhanced permeability through rat skin. *J Colloid Interface Sci*. 2008;318(2):421–429. doi:10.1016/j.jcis.2007.10.036
33. Sakdiset P, Okada A, Todo H, Sugibayashi K. Selection of phospholipids to design liposome preparations with high skin penetration-enhancing effects. *J Drug Deliv Sci Technol*. 2018;44:58–64. doi:10.1016/j.jddst.2017.11.021
34. Yang X, Xu L, Zhou J, et al. Integration of phospholipid-complex nanocarrier assembly with endogenous N-oleoylethanolamine for efficient stroke therapy. *J Nanobiotechnology*. 2019;17(1). doi:10.1186/s12951-019-0442-x
35. Nones J, Riella HG, Trentin AG, Nones J. Effects of bentonite on different cell types: a brief review. *Appl Clay Sci*. 2015;105–106:225–230. doi:10.1016/j.clay.2014.12.036
36. Maisanaba S, Gutiérrez-Praena D, Pichardo S, et al. Toxic effects of a modified montmorillonite clay on the human intestinal cell line Caco-2. *J Appl Toxicol*. 2014;34(6):714–725. doi:10.1002/jat.2945
37. Ghyczy M, Vacata V. Phosphatidylcholine and skin hydration. In: *Skin Moisturization*. CRC Press; 2002:303–321. doi:10.3109/9780203908235-19
38. Maxim LD, Niebo R, McConnell EE. Bentonite toxicology and epidemiology – a review. *Inhal Toxicol*. 2016;28(13):591–617. doi:10.1080/08958378.2016.1240727